Effect of Temperature on Polyelectrolyte Expansion of Lignosulfonate

Hao Li,[a] Yonghong Deng,[a,]* Huangqing Ye,[a] Liang Xiao,[a] and Xueqing Qiu [a,b,]*

The temperature effect on the polyelectrolyte expansion of sodium lignosulfonate (SL) was studied in the range of 20 to 38 °C. A narrow molecular-weight distribution fraction of sodium lignosulfonate was first obtained by gel column chromatography, which was suitable for the hydrodynamic radius (R_h) measurement by dynamic light scattering (DLS). Dynamic light scattering experiments showed that the hydrodynamic radius of sodium lignosulfonate decreased with increasing temperature. Using a quartz crystal microbalance (QCM) and atomic force microscopy (AFM), it was found that the adsorbed sodium lignosulfonate film lost water with increasing temperature and reabsorbed water with decreasing temperature. Surface tension and contact angle experiments showed that there were more hydrophobic groups on the surface of the sodium lignosulfonate molecule as the temperature increased. It can be concluded that the sodium lignosulfonate molecule shrank and became more hydrophobic with increasing temperature. Analysis suggests that the decreasing of the hydrogen-bond interactions between the sodium lignosulfonate molecule and water molecules with increasing temperature is the primary reason for the molecular conformation change of sodium lignosulfonate.

Keywords: Sodium lignosulfonate; Temperature; Polyelectrolyte expansion; Molecular conformation

Contact information: a: School of Chemistry and Chemical Engineering, South China University of Technology, 381 Wushan Road, Guangzhou, 510640, China; b: State Key Lab of Pulp & Paper Engineering, South China University of Technology, 381 Wushan Road, Guangzhou, 510640, China;
** Corresponding authors: yhdeng08@163.com; xueqingqiu66@163.com*

INTRODUCTION

Sodium lignosulfonate (SL), a renewable anionic polyelectrolyte, is the primary component in the spent liquors of the sulfite pulping process. Although the exact structure of sodium lignosulfonate has not been elucidated, it is widely accepted that SL is a kind of three-dimensional cross-linked biopolymer that contains both hydrophilic groups (sulphonic, carboxylic, phenylic hydroxyl, and alcoholic hydroxyl) and hydrophobic groups (aromatic, aliphatic, and carbon chains). Because of the coexistence of hydrophilic and hydrophobic groups, SL has a surface activity that promotes surface adsorption and further particle dispersion ability. Therefore, SL has found widespread practical applications because of its dispersing properties, such as a dispersant for concrete (Miyake *et al.* 1985; Grierson *et al.* 2005; Ouyang *et al.* 2006a; Yu *et al.* 2013), coal-water slurries (Yang *et al.* 2007), ceramic slurries (Ratinac *et al.* 2004; Li *et al.* 2013), pesticides (Li *et al.* 2009; Pang *et al.* 2014), dyestuff (Lin 1982), and recirculating cooling water (Ouyang *et al.* 2006b).

Expanding the applications of SL requires a better understanding of its polyelectrolyte properties. In previous research, the polyelectrolyte expansion of SL was shown to be influenced by ionic strength (Rezanowich and Goring 1960) and pH value (Deng *et al.* 2010; Yan *et al.* 2010; Qian *et al.* 2011). However, the temperature effect on the polyelectrolyte expansion properties of SL still has not been studied by researchers.

Most applications of SL involve temperature variation. For example, a change in temperature would accompany the heat-release of cement hydration (Grierson *et al.* 2005; Pang *et al*. 2005), as well as the recirculating cooling water system (Ouyang *et al.* 2006b) and the dyeing process (Lin 1982). Moreover, many applications of SL dispersants during construction are out of doors, so the temperature conditions of these applications would depend on the atmospheric temperature. Thus, the performance of SL may be influenced by changes in temperature. It is generally believed that the performance of SL partly depends on its molecular conformation, which is related to the electrostatic repulsion (Zhou *et al.* 2012) and steric hindrance (Li *et al.* 2011) of the particle surface. Therefore, research on the influence of temperature on the molecular conformations of SL is fundamental to its application.

There are several reports on the influence of temperature on the molecular conformations of polyelectrolytes. However, the molecular conformations of different polyelectrolytes present various features with increasing temperature. For example, polyelectrolytes such as poly(N-isopropylacrylamide) (Wang and Wu 1998; Liu and Zhang 2004; Ishida and Biggs 2007) and poly(styrene sulfonate) (Nestler *et al.* 2012) shrink and tend to collapse to dense globules with extended chain conformations; meanwhile, others such as phospholipids (Ariga and Okahata 1994), poly(diallyldimethylammonium chloride) (Tan *et al.* 2003), and poly(allylamine hydrochloride) (Nestler *et al.* 2012) expand when the temperature increases. It seems that there is no uniform criterion for predicting the influence of temperature on the conformation changes of polyelectrolytes, especially for SL, because it has an extremely complex molecular structure that is still undefined. Moreover, SL is a colloidal polyelectrolyte with an oblate spheroid shape (Vainio *et al.* 2008), so it may have extraordinary characteristics that are different from common polyelectrolytes. Even the different lignin derivatives that all come from the chemical modification of lignin have different temperature responsive properties (Deng *et al.* 2014). Therefore, it is necessary to carry out special research concerning the effect of temperature on the conformation changes of SL.

There are very few reports on the effect of temperature on the molecular conformation of SL. Studies by Vainio *et al.* (2008) and Qian *et al.* (2014) both determined that SL can aggregate at high temperature. Moreover, the effect of temperature on the effective charge numbers and diffusion coefficients of LS was studied by Mafé *et al*. (1995). But there are no descriptions that include the polyelectrolyte expansion behavior of SL. Moreover, from the results of simulation analysis, Petridis *et al.* (2011) conclude that lignin can transition from compact conformations to extended conformations with increasing temperature. However, logically, if the SL molecule conformation can extend with increasing temperature, then the solubility of the SL molecule will increase at high temperature. With better solubility conditions, SL may not aggregate with increasing temperature. Therefore, the simulated lignin model may not be suitable for directly predicting the behavior of SL. Currently, there is still no direct experimental evidence to reveal this phenomenon. However, it may be possible to determine whether the molecular conformation of SL is shrinking or expanding with increasing temperature by studying the changes of its hydrodynamic radius distribution and some other physicochemical behaviors.

In a previous paper, the authors confirmed that SL molecules can form intermolecular aggregates at the critical temperature of 38 °C (Qian *et al.* 2014). This manuscript reports the further study of how the molecular conformation changes of SL are influenced by temperature. However, both of the conformations of single molecules and aggregates would change with increasing temperature. As a consequence, the information obtained by the instruments for revealing the conformation changes of the single molecules may be affected by the aggregates factor. Thus the conformational changes affected by temperature studied in a larger temperature interval can't be not revealed clearly (Qiu *et al.* 2012). This means that studying single molecules and aggregates in solution at the same time is very complex. In order to provide precise research on the expansion behaviors of SL with temperature, the range 20 to 38 °C was selected, because there are no SL aggregates in this range. Meanwhile, to ensure the accuracy of the results in the dynamic light scattering (DLS) experiment, a SL fraction with a narrow molecular-weight distribution, obtained by gel column chromatography (Ouyang *et al.* 2011), was used for the hydrodynamic radius measurement. To reveal how the hydration behavior of SL is influenced by the temperature, the SL was first modified with sulfhydryl to form a steady SL adsorbed film on gold quartz crystal; then, the changes in water amount in the already-formed SL film with temperature were monitored by quartz crystal microbalance (QCM). Moreover, the surface morphologies of the SL adsorption films at different temperatures were detected by atomic force microscopy (AFM) to provide visual images of the molecular conformation changes. In addition, the surface tension of the solution and the static contact angle of the SL adsorption films influenced by temperature were also studied to obtain in-depth knowledge of the effect of temperature on the conformation changes of SL. The related results can give a better understanding of the conformational features of the SL molecule with respect to temperature.

EXPERIMENTAL

Materials

Raw SL was obtained from Shixian Papermaking Co. Ltd. (China) as a byproduct of sulfite pulping. Before the experiment, the commercial SL was first filtered to remove the insoluble solid matter, and the low-molecular weight (M_w) impurities were then removed using an ultrafiltration apparatus (Wuxi Membrane Science and Technology Co., China) with a 2500-Da cutoff membrane. The material obtained by ultrafiltration was then fractionated using gel column chromatography. The details of the gel column chromatography process has been described in previous papers (Ouyang *et al.* 2011; Deng *et al.* 2012). A fraction with a weight-average M_w of ~58,000 g/mol and a polydispersity index (M_w/M_n) of ~1.4 was used in this experiment, and these molecular weight parameters were determined by gel permeation chromatography (GPC) according to the methods described in Ouyang *et al.* (2011). The concentration of this fraction is 0.3064 g/L, as determined by a UV-vis spectrophotometer (UV-2550; Shimadzu Co., Japan).

To prepare SL for adsorption on gold-coated quartz crystal, SL was first modified with sulfhydryl groups to form a thiol-gold bond with Au. A strong thiol-gold bond was formed between the sulfhydryl groups and the Au with a bond energy of 40 kJ/mol (Hasan *et al.* 2002). When the sulfhydryl-modified SL, named HS-SL, is adsorbed on the Au-coated quartz crystal, the bond is difficult to break by a change in solution conditions (Love *et al.* 2005). The HS-SL was synthesized using purified SL and mercaptoacetic acid, in which the alcoholic hydroxyl groups of SL are subjected to an esterification reaction with the carboxyl groups of mercaptoacetic acid (Xie and Zeng 2006) as described in Scheme 1. The esterification reaction in this experiment was performed using the following procedure. Approximately 15 mL of a mixture composed of five parts of sulfuric acid (98%) and 10 parts (v/v) of SL was added to about 25 mL of SL aqueous solution (10%) in a 100-mL round-bottom flask. The flask was sealed and placed in a water bath at 80 °C for 6 h with continuous magnetic stirring. After the reaction finished, the residual liquid was treated by dialysis for 24 h to remove the excessive sulfuric acid and mercaptoacetic acid. The water in the solution was then evaporated in a rotary evaporator at a temperature of 50 °C. The residue, *i.e.*, the HS-SL, was stored in a drier away from light until it was used in the experiments.

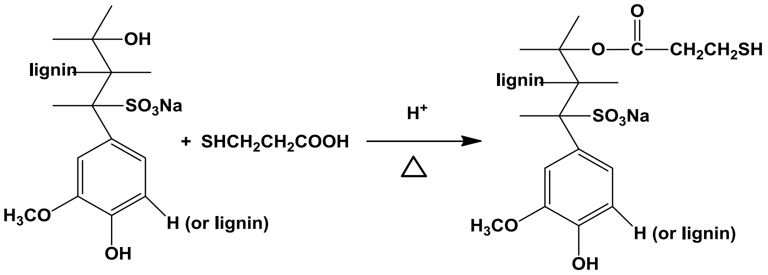

Scheme 1. Schematic diagram of HS-SL synthesis

All other solvents and reagents were purchased commercially as analytical grade products and used directly without further purification.

Methods

Laser light scattering was performed on a commercial light scattering spectrometer (ALV/CGS-3, ALV, Germany) equipped with a multi-τ digital time correlator (ALV-7004, ALV, Germany) and a cylindrical 22-mW Uniphase He-Ne laser (λ_0=632 nm) as the light source. A 632.8-nm interference filter and a Glan-Thompson interferometer were used to avoid overestimation of the laser intensity of SL due to fluorescence and polarization. The R_h of the SL molecule was calculated from the Laplace inversion of $G^2(t)$ using the CONTIN software. For the purpose of dust removal, the solutions were filtered with 0.45-μm PVDF Millipore Millex-LRC filters before the light scattering analysis.

The surface tension was measured using a Wilhelmy plate with a dynamic contact angle meter from Dataphysics Instruments Co., Ltd. (Germany). Experimental errors inherent in the measurement were ±0.03 mN/m. The surface tension was determined as an average value of three measurements at each temperature.

The QCM-D measurements were performed using a Q-Sense E1 instrument (Q-Sense AB Corp., Sweden). Upon interaction of matter with the surface of a sensor crystal, changes in the resonance frequency, Δ*f*, related to the attached mass (including coupled water) in the ad-layer were measured. Changes in frequency of the third overtone are presented here. The temperature was controlled in the range of ± 0.02 °C.

The AFM images and surface roughness of the SL adsorption films were obtained using a XE-100 (Park Systems, Korea) instrument in non-contact mode and a PPP-NCHR cantilever. All images presented are height images and have been zero-order flattened using a standard algorithm within the XEI software to remove the artificial height offsets between consecutive scan lines of the raw images.

The static contact angles of the SL adsorption films were measured using a JC2000C1 contact angle tester (Zhongchen Digital Technic Apparatus Co., Ltd., China). The contact angle was determined as an average value of three measurements at each condition.

RESULTS AND DISCUSSION

Polyelectrolyte Expansion of SL in Solution with Temperature

The hydrodynamic radius distribution (R_h) of the SL molecule in solution is the primary characteristic determining its polyelectrolyte expansion behavior. The R_h changes of SL at different temperatures were measured by dynamic light scattering (DLS) first. The changes in the R_h distributions of SL as the temperature increased from 20 to 38 °C are shown in Fig. 1a; the relationship between the average R_h and temperature is shown in Fig. 1b. It is obvious that R_h decreased with increasing temperature in the range of 20 to 38 °C and increased again when the temperature decreased. Although the average R_h in the cooling process was unable to completely recover to the original state immediately, it still gradually reached the initial state after a longer period of time (inset in Fig. 1b). The changes to R_h clearly indicate that SL shrank with increasing temperature and expanded with decreasing temperature. In spite of some hysteresis, the shrinking and expanding process appears to be reversible.

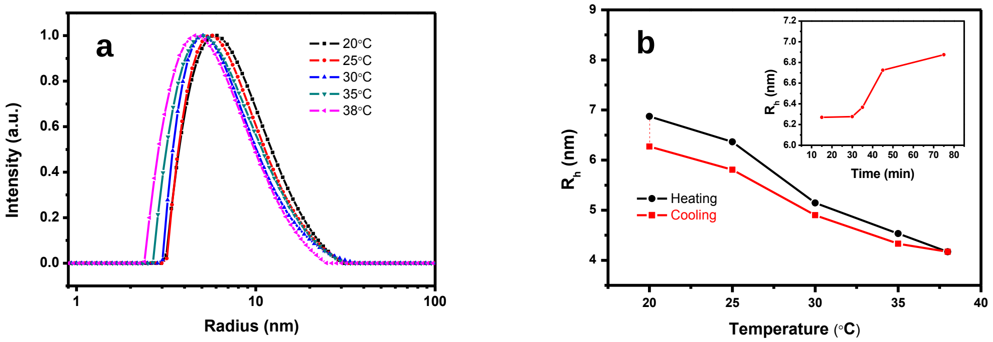

Fig.1. (a) R_h distributions of SL at different temperatures; (b) Temperature dependence of the average R_h in the heating and cooling processes, each point was obtained at 15 min after the solution reached the thermal equilibrium. Inset: time dependence of average R_h after the temperature cooling to 20 °C in the cooling processes

It is well known that the properties of the surface groups of the surfactant molecules or surfactant micelles are the principal factors affecting the solution surface tension (Eastoe *et al*. 2000). And it has also been found that SL with more hydrophobic groups has a lower surface tension (Ge *et al*. 2014). Therefore, in addition to the changes in R_h, the variations in surface tension with temperature could also reflect the conformational changes in SL to a certain extent. Figure 2 shows the temperature dependence of the surface tension for a 1g/L SL solution. For comparison, the surface tension of pure water was also measured as a blank, and it can be seen that the surface tension of the SL solution decreased more quickly than that of pure water. Other studies have shown that the surface tension of small-molecule surfactant solutions decreases with increasing temperature, but the decrease is very small. For example, when the temperature rises from 20 to 38 °C, the surface tensions of cetrimonium bromide solution and sodium dodecyl sulfate solution decreased by only 2 to 3 mN/m (Du *et al.* 2006). However, the decrease in the surface tension of the SL solution in the same temperature range is about 10.7 mN/m. This result must be caused by the significant conformational changes of the SL molecule when the temperature increases. From these results, it can be concluded that there are more hydrophobic groups exposed to the air/liquid interface with increasing temperature; for this reason, the hydrophobicity of the SL molecule increases. One can conclude that the shrinking process of the SL molecule is also accompanied by the enhancement of hydrophobicity.

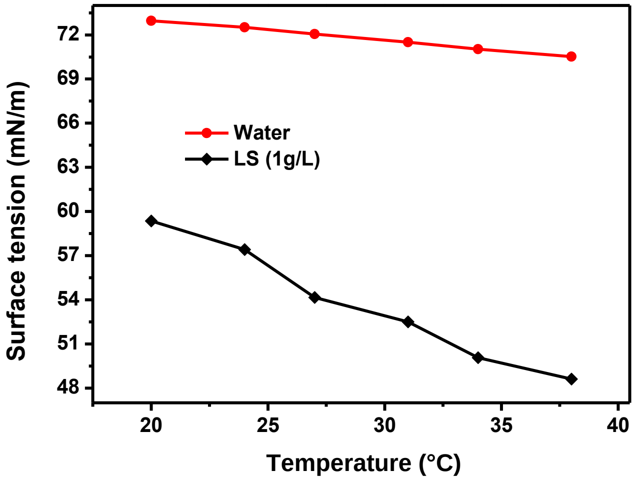

Fig. 2. Surface tension of LS solution (1g/L) at different temperatures. For comparison, the surface tension of pure water was measured as a blank

Polyelectrolyte Expansion of SL Adsorption Film in Water

To further study the shrinkage of the SL molecule with increasing temperature, the changes to the SL molecule conformation in the adsorption film were investigated by QCM. The adsorption process of HS-SL on an Au-coated sensor crystal at 20 °C was first characterized; the results are shown in Fig. 3.

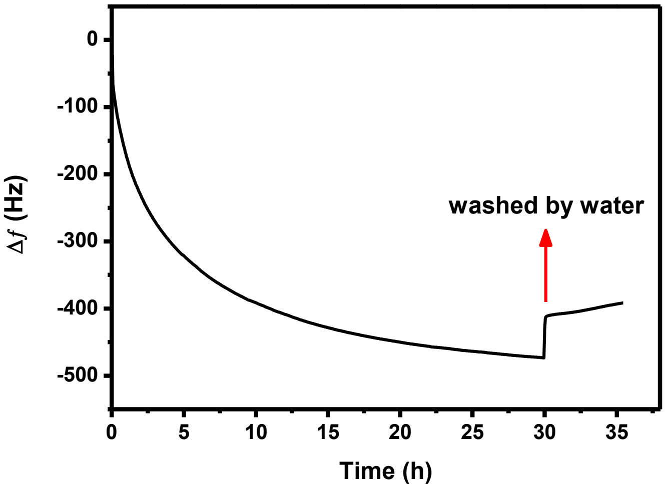

Fig. 3. Δ*f* as a function of time for HS-SL adsorbed onto a gold-coated quartz crystal (n=3). The concentration of the HS-SL solution used was 1g/L. Arrows indicate the start of surface rinsing with Milli-Q water. All of the related operations were conducted at 20 °C

It is clear that Δ*f* decreased quickly with time, which indicates that more and more HS-SL molecules were adsorbed on the Au surface. When the HS-SL adsorption process on Au surface was complete, the HS-SL film was rinsed with Milli-Q water. Most of the HS-SL still remained on the gold quartz crystal, even though it was rinsed with large quantities of water. The firm adsorption state lays the foundation for the study of hydration behavior by QCM. After rinsing, the HS-SL film on the Au surface was used to investigate the molecular conformation changes of SL with temperature.

When the frequency reached a stable state after the HS-SL adsorption film was rinsed with water, the frequency was reset to zero so that the state of the SL film was defined as a reference. Figure 4a shows Δ*f* changes in the HS-SL film-coated Au in water at different temperatures. The changes in frequency come not only from the HS-SL film, but also from the crystal resonator itself and the water surrounding them, as the viscosity and density of water also change with temperature (Liu and Zhang 2004; Ishida and Biggs 2007). Therefore, for comparison, changes in Δ*f* for bare Au in water at different temperatures are also shown in Fig. 4a.

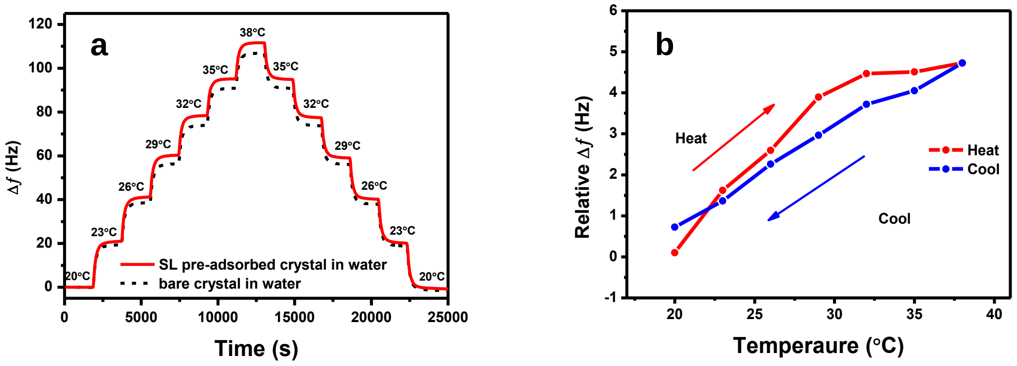

Fig. 4. (a)Δf of a bare gold quartz crystal (dashed line) and HS-SL adsorbed onto a gold quartz crystal (solid line) (n=3). The temperature changed with time. (b) Temperature dependence of Δf of as-formed SL film (n=3)

For both the bare and the HS-SL adsorbed sensor crystal, the frequencies increased with increasing temperature and decreased with decreasing temperature. Compared with the Δ*f* of bare Au in water, the HS-SL-coated Au exhibited a larger increment with increasing temperature. In Fig. 4b, the relative Δ*f* changes of the as-formed SL film at each temperature were evaluated by subtracting the Δ*f* change values of the bare crystal resonator. The relative Δ*f* gradually increased with increasing temperature, which means that some water molecules were removed from the as-formed HS-SL film. This may indicate that, as temperature increases, dehydration occurs and SL molecules gradually shrink, accompanied by water release. Conversely, the collapsed SL film became swollen with decreasing temperature in the cooling process, as reflected in the decreasing relative Δ*f*.

The AFM images of the as-formed SL films on gold at two different temperatures are shown in Fig. 5, in which the two pictures have the same length scale. At 20 °C, the film appeared relatively flat, and only weak structural features could be seen. When the temperature was increased to 38 °C, a large number of rough structures became clearly visible on the surface. This coarse structure consisted of protuberances and holes and was not as homogeneous as it was at the lower temperature.

The changes in the observed structures from the two images can be further analyzed numerically using the rms (root-mean-square) roughness from each image. As Table 1 shows, the roughness values obtained were 0.927 and 1.552 nm at 25 and 38 °C, respectively. The roughness values also indicate that the dehydration and collapse of the molecules occurs as the temperature increases. Here, the result of AFM images is consistent with the conclusion drawn from the QCM, and it can be further confirmed that increasing temperature can cause the molecule to shrink.

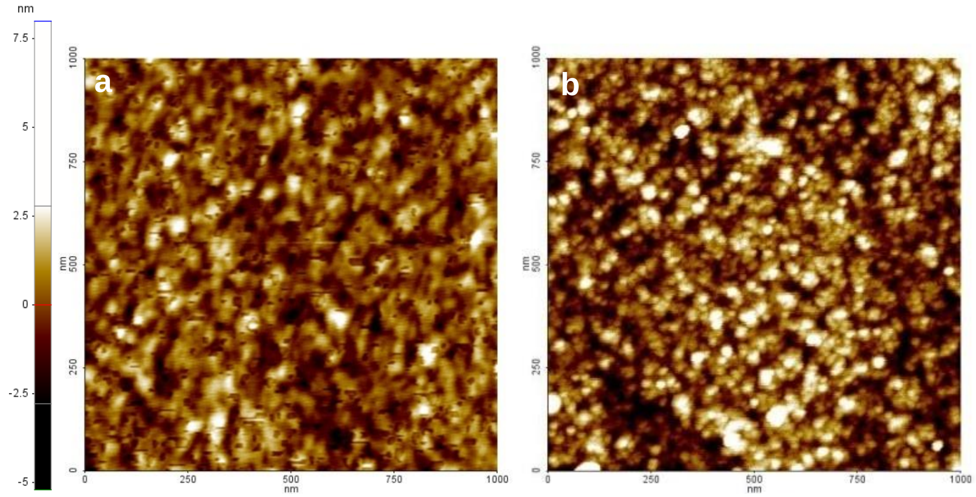

Fig. 5. AFM images of HS-SL adsorption films at two different temperatures: (a) 20 °C (b) 38 °C

Table 1. Surface Properties of SL Adsorption Films at Two Different Temperatures

Sample	20°C	38°C
Rms(nm)	0.927	1.552
Contact angle (°)	59.5	62.5

The surface wettability of the adsorption films can be detected by measuring the contact angle. The smaller the contact angle, the more wettable the surface. Table 1 shows the contact angle of the SL adsorption films at two different temperatures. Generally speaking, for the same hydrophilic surfaces, a larger roughness results in a smaller contact angle (Chen *et al.* 1999). However, the adsorbed film formed at 38 °C, which had a larger roughness, presented a larger contact angle. This means that the adsorbed film formed at 38 °C had a more hydrophobic surface. Therefore, it can also be concluded that there was a higher proportion of hydrophobic groups on the surface of SL molecules with increasing temperature. This conclusion is consistent with the results of the surface tension experiment. Both of them indicate that the SL molecule became more hydrophobic with increasing temperature.

Molecular Shrinkage Mechanism with Increasing Temperature

In the SL molecules, there are many hydrophilic groups, such as carboxylic, ether, phenylic hydroxyl, and alcoholic hydroxyl groups, and these groups can form hydrogen bonds with water molecules in solution. A change in temperature can have a remarkable influence on the hydrogen interactions between the hydrophilic groups and the water molecules, as suggested in Fig. 6. Because of the complex structure of SL, only a schematic illustration for the surface area of the SL molecule is shown in Fig. 6.

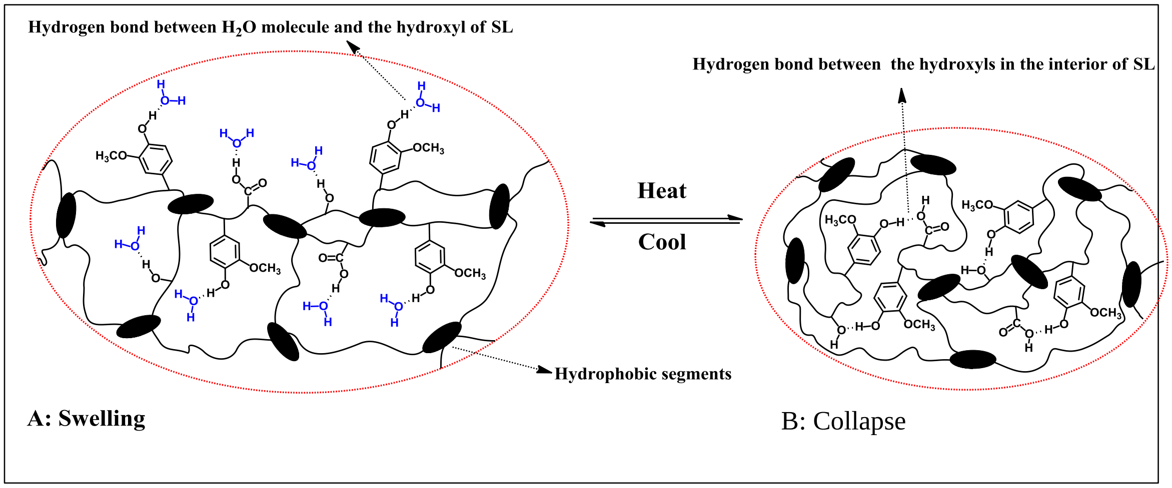

Fig. 6. Schematic illustration of the shrinking and expanding mechanism of SL; only partial enlarged drawings of the SL molecular surface area is shown here. In state A, SL forms more hydrogen bonds with H_2O; in state B, some hydrogen bonds between LS and H_2O are broken and more hydrogen bonds between the hydroxyls in the interior of SL are formed. Accompanied by intramolecular aggregates, some hydrophilic groups initially on the surface get into the interior of the SL molecule

As shown in Fig. 6, at lower temperatures, there are more hydrogen bond combinations between the water molecules and the hydrophilic groups of SL. For this reason, there is a solvation layer connected by hydrogen bonds around the SL molecule, which makes the conformation of SL more expanded. As the temperature increases, some of the hydrogen bonds between the water molecules and the hydrophilic groups in SL are broken. Therefore, more intramolecular hydrogen bonds are formed between the hydroxyl, ether, and carboxyl groups, leading to intramolecular aggregation. Accompanied by the formation of intramolecular hydrogen bonds, some hydrophilic groups that were initially on the surface get into the interior of the SL molecule, leaving a higher proportion of hydrophobic groups at the surface and increasing the hydrophobicity of the SL molecule. As a consequence of these changes, the hydrophilic groups lose the water molecules that are initially bounded to them and the SL macromolecule is collapsed. In the shrinking process, some hydrophilic groups that are initially at the surface can get into the interior of the SL molecule, leaving a higher proportion of hydrophobic groups on the surface. Therefore, at higher temperatures, the SL molecule not only appears to be in a more shrinking state but also becomes more hydrophobic. The formation of intra-chain structures in the shrinking state would persist in the shrinking-to-expanding transition. Therefore, a hysteresis was observed in the cooling process.

CONCLUSIONS

1. In the investigated temperature range of 20 to 38 °C, with increasing temperature, the molecular conformation of SL in solution appears to shrink. Although there is some hysteresis, the shrinking and expanding process is reversible.
2. The SL adsorption film loses water with increasing temperature and reabsorbed water with decreasing temperature. This result appears to be complementary and shows a fair correlation with the behavior of the SL molecule in solution.
3. The analysis suggests that the effect of temperature on the expansion of SL is primarily realized by affecting the hydrogen-bond interactions between the SL molecule and water molecules. With increasing temperature, some of the hydrogen bonds between LS and H_2O are broken, and more intramolecular hydrogen bonds within the SL molecule are formed, leading to intramolecular aggregates.
4. Accompanied by the formation of intramolecular hydrogen bonds, more hydrophilic groups get into the interior of the SL molecule, leaving a higher proportion of hydrophobic groups at the surface, which enhances the hydrophobicity of SL at higher temperature.

ACKNOWLEDGMENTS

The authors are grateful for the financial support of the National Basic Research Program of China (973 Program) (2012CB215302) and the National Natural Science Foundation of China (21374032).

REFERENCES CITED

Ariga, K., and Okahata, Y. (1994). “Hydration behavior of phospholipid Langmuir-Blodgett (LB) films deposited on a quartz-crystal microbalance depending on temperatures in water,” *Langmuir* 10(7), 2272-2276. DOI: 10.1021/la00019a041

Chen, W., Fadeev, A. Y., Hsieh, M. C., Öner, D., Youngblood, J., and McCarthy, T. J. (1999). “Ultrahydrophobic and ultralyophobic surfaces: Some comments and examples,” *Langmuir* 15(10), 3395-3399. DOI: 10.1021/la990074s

Deng, Y., Wu, Y., Qian, Y., Ouyang, X., Yang, D., and Qiu, X. (2010). “Adsorption and desorption behaviors of lignosulfonate during the self-assembly of multilayers,” *BioResources* 5(2), 1178-1196. DOI: 10.15376/biores.5.2.1178-1196

Deng, Y., Feng, X., Yang, D., Yi, C., and Qiu, X. (2012). “Pi-pi stacking of the aromatic groups in lignosulfonates,” *BioResources* 7(1), 1145-1156. DOI: 10.15376/biores.7.1.1145-1156

Deng, Y., Guo, Y., Qian,Y., Lou, H., and Qiu, X. (2014). “Effect of temperature on a lignin-based polymer with two types of microstructures,” *BioResources* 9(4), 6304-6315. DOI: 10.15376/biores.9.4.6304-6315

Du, B., Tang, Y., Yang, J., and Zhang, Y. (2006). “Surface tension and emulsifiability of aqueous equimolar CTAB-SDS mixture at different temperatures,” *Fine Chemicals* 23(1), 25-27.

Eastoe, J., and Dalton, J. S. (2000). "Dynamic surface tension and adsorption mechanisms of surfactants at the air-water interface," *Advances in Colloid and Interface Science* 85(2-3), 103-144. DOI:10.1016/S0001-8686(99)00017-2

Ge, Y., Li, D., and Li, Z. (2014). "Effects of lignosulfonate structure on the surface activity and wettability to a hydrophobic powder" *BioResources* 9(4), 7119-7127.

Grierson, L. H., Knight, J. C., and Maharaj, R. (2005). "The role of calcium ions and lignosulphonate plasticiser in the hydration of cement," *Cement and Concrete Research* 35(4), 631-636. DOI: 10.1016/j.cemconres.2004.05.048

Hasan, M., Bethell, D., and Brust, M. (2002). "The fate of sulfur-bound hydrogen on formation of self-assembled thiol monolayers on gold: ^{1}H NMR spectroscopic evidence from solutions of gold clusters," *Journal of the American Chemical Society* 124(7), 1132-1133.DOI: 10.1021/ja0120577

Ishida, N., and Biggs, S. (2007). "Direct observation of the phase transition for a poly(n-isopropylacryamide) layer grafted onto a solid surface by AFM and QCM-D," *Langmuir* 23(22), 11083-11088. DOI: 10.1021/la701461b

Li, Z., Pang, Y., Lou, H., and Qiu, X. (2009). "Influence of lignosulfonates on the properties of dimethomorph water-dispersible granules," *BioResources* 4(2), 589-601. DOI: 10.15376/biores.4.2.589-601

Li, Z., Pang, Y., Ge, Y., and Qiu, X. (2011). "Evaluation of steric repulsive force in the aqueous dispersion system of dimethomorph powder with lignosulfonates via X-ray photoelectron spectroscopy," *The Journal of Physical Chemistry C* 115(50), 24865-24870. DOI: 10.1021/jp2083117

Li, R., Yang, D., Guo, W., and Qiu, X. (2013). "The adsorption and dispersing mechanisms of sodium lignosulfonate on Al_2O_3 particles in aqueous solution," *Holzforschung* 67(4), 387-394. DOI: 10.1515/hf-2012-0108

Lin, S. Y. (1982). "Method for polymerization of lignosulfonates," *United States Patent* 4,332,589.

Liu, G., and Zhang, G. (2004). "Collapse and swelling of thermally sensitive poly(N-isopropylacrylamide) brushes monitored with a quartz crystal microbalance," *The Journal of Physical Chemistry B* 109(2), 743-747. DOI: 10.1021/jp046903m

Love, J. C., Estroff, L. A. Kriebel, J. K., Nuzzo, R. G., and Whitesides, G. M. (2005). "Self-assembled monolayers of thiolates on metals as a form of nanotechnology," *Chemical Reviews* 105(4), 1103-1170. DOI: 10.1021/cr0300789

Mafé, S. Manzanaresa, J., Kontturib, A., and Kontturib, K. (1995). "Temperature effects on counterion binding to spherical polyelectrolytes: The charge-discharge transition of lignosulfonate," *Bioelectrochemistry and Bioenergetics* 38(2), 367-375. DOI:10.1016/0302-4598(95)01814-U

Miyake, N., Ando, T., and Sakai, E. (1985). "Superplasticized concrete using refined lignosulfonate and its action mechanism," *Cement and Concrete Research* 15(2), 295-302. DOI: 10.1016/0008-8846(85)90041-9

Nestler, P., Block, S., and Helm, C.A. (2012). "Temperature-induced transition from odd-even to even-odd effect in polyelectrolyte multilayers due to interpolyelectrolyte interactions," *The Journal of Physical Chemistry B* 116(4), 1234-1243. DOI: 10.1021/jp208837m

Ouyang, X., Qiu, X., and Chen, P. (2006a). "Physicochemical characterization of calcium lignosulfonate - A potentially useful water reducer," *Colloids and Surfaces A-Physicochemical and Engineering Aspects* 282-283(20), 489-497. DOI: 10.1016/j.colsurfa.2005.12.020

Ouyang, X., Qiu, X., Lou, H., and Yang, D. (2006b). "Corrosion and scale inhibition properties of sodium lignosulfonate and its potential application in recirculating cooling water system," *Industrial & Engineering Chemistry Research* 45(16), 5716-5721. DOI: 10.1021/ie0513189

Ouyang, X., Zhang, P., Qiu, X., Deng, Y., and Chen, P. (2011). "Lignosulfonate separation using preparative column chromatography," *Industrial & Engineering Chemistry Research* 50(16), 10792-10799. DOI: 10.1021/ie0513189

Pang, Y., Qiu, X., and Yang, D. (2005). "Influence of calcium lignosulfonate on cement hydration," *Journal of the Chinese Ceramic Society* 33(4), 477-483.

Pang, Y., Gao, W., Lou, H., Zhou, M., and Qiu, X. (2014). "Influence of modified lignosulfonate GCL4-1 with different molecular weight on the stability of dimethomorph water based suspension," *Colloids and Surfaces A: Physicochemical and Engineering Aspects* 441(20), 664-668. DOI: 10.1016/j.colsurfa.2013.10.014

Petridis, L., Schulz, R., and Smith, J. C. (2011). "Simulation analysis of the temperature dependence of lignin structure and dynamics," *Journal of The American Chemical Society* 133(50), 20277-20287. DOI: 10.1021/ja206839u

Qian, Y., Deng, Y., Yi, C., Yu, H., and Qiu, X. (2011). "Solution behaviors and adsorption characteristics of sodium lignosulfonate under different pH conditions," *BioResources* 6(4), 4686-4695. DOI: 10.15376/biores.6.4.4686-4695

Qian, Y., Deng, Y., Qiu, X., Huang, J., and Yang, D. (2014). "Aggregation of sodium lignosulfonate above a critical temperature," *Holzforschung* 68(6), 641-647. DOI: 10.1515/hf-2013-0167

Qiu, X., Qian, Y., Guo, Y., and Deng, Y. (2012). "Molecular configuration fitting of sodium lignosulfonate in aqueous solution," *Journal of South China University of Technology (Natural Science Edition)* 40(10), 77-82. DOI: 10.3969/j.issn.1000-565X.2012.10.010

Ratinac, K. R., Standard, O. C., and Bryant, P. J. (2004). "Lignosulfonate adsorption on and stabilization of lead zirconatetitanate in aqueous suspension," *Journal of Colloid and Interface Science* 273(2), 442-454. DOI: 10.1016/j.jcis.2004.02.044

Rezanowich, A., and Goring, D. A. I. (1960). "Polyelectrolyte expansion of a lignin sulfonatemicrogel,"*Journal of Colloid Science* 15(5), 452-471. DOI: 10.1016/0095-8522(60)90049-0

Tan, H. L., McMurdo, M. J., Pan, G., and Van Patten, P. G. (2003). "Temperature dependence of polyelectrolyte multilayer assembly," *Langmuir* 19(22), 9311-9314. DOI: 10.1021/la035094f

Vainio, U., Lauten, R. A., and Serimaa, R. (2008). "Small-angle X-ray scattering and rheological characterization of aqueous lignosulfonate solutions," *Langmuir* 24(15), 7735-7743. DOI: 10.1021/la800479k

Wang, X., and Wu, C. (1998). "Globule-to-coil transition of a single homopolymer chain in solution," *Physical Review Letters* 80(18), 4092-4094. DOI: 10.1103/PhysRevLett.80.4092

Xie, Y., and Zeng, X. (2006). "Preparation of sulfhydryl-lignin and its adsorbing heavy metal ions," *Technology of Water Treatment* 32(6), 73-74.

Yan, M., Yang, D., Deng, Y., Chen, P., Zhou, H., and Qiu, X. (2010). "Influence of pH on the behavior of lignosulfonate macromolecules in aqueous solution," *Colloids and Surfaces A: Physicochemical and Engineering Aspects* 371(1-3), 50-58. DOI: 10.1016/j.colsurfa.2010.08.062

Yang, D., Qiu, X., Zhou, M., and Lou, H. (2007). "Properties of sodium lignosulfonate as dispersant of coal water slurry," *Energy Conversion and Management* 48(9), 2433-2438. DOI: 10.1016/j.enconman.2007.04.007

Yu, G., Li, B., Wang, H., Liu, C., and Mu, X. (2013). "Preparation of concrete superplasticizer by oxidation-sulfomethylation of sodium lignosulfonate," *BioResources* 8(1), 1055-1063. DOI: 10.15376/biores.8.1.1055-1063

Zhou, H., Yang, D., Wu, X., Deng, Y., and Qiu, X. (2012). "Physicochemical properties of sodium lignosulfonates (NaLS) modified by laccase," *Holzforschung* 66(7), 825-832.DOI: 10.1515/hf-2011-0189

Article submitted: August 10, 2014; Peer review completed: November 12, 2014; Revised version received: November 16, 2014; Accepted: November 7, 2014; Published: November 26, 2014.